

WASHINGTON UNIVERSITY
DEPARTMENT OF PHYSICS
LABORATORY FOR ULTRASONICS
St. Louis, Missouri 63130

"Physical Interpretation and Development of Ultrasonic Nondestructive
Evaluation Techniques Applied to the Quantitative Characterization of Textile
Composite Materials"

Semiannual Progress Report: September 15, 1993 - March 14, 1994

NASA Grant Number: NSG-1601

Principal Investigator:

Dr. James G. Miller
Professor of Physics

The NASA Technical Officer for this grant is:

Dr. Joseph S. Heyman
NASA Langley Research Center
Hampton, Virginia

N94-30016

Unclas

0003922

(NASA-CR-195766) PHYSICAL
INTERPRETATION AND DEVELOPMENT OF
ULTRASONIC NONDESTRUCTIVE
EVALUATION TECHNIQUES APPLIED TO
THE QUANTITATIVE CHARACTERIZATION
OF TEXTILE COMPOSITE MATERIALS
Semiannual Progress Report, 15 Sep. 63/24
1993 - 14 Mar. 1994 (Washington
Univ.) 19 p

11-24-CR
3922
198

**ORIGINAL CONTAINS
COLOR ILLUSTRATIONS**

Introduction

In this Progress Report, we describe our continuing research activities concerning the development and implementation of advanced ultrasonic nondestructive evaluation methods applied to the inspection and characterization of complex composite structures. We explore the feasibility of implementing medical linear array imaging technology as a viable ultrasonic-based nondestructive evaluation method to inspect and characterize complex materials. As an initial step toward the application of linear array imaging technology to the interrogation of a wide range of complex composite structures, we present images obtained using an unmodified medical ultrasonic imaging system of two epoxy-bonded aluminum plate specimens, each with intentionally disbanded regions. These images are compared with corresponding conventional ultrasonic contact transducer measurements in order to assess whether these images can detect disbanded regions and provide information regarding the nature of the disbanded region.

We present a description of a standoff/delay fixture which has been designed, constructed, and implemented on a Hewlett-Packard SONOS 1500 medical imaging system. This standoff/delay fixture, when attached to a 7.5 MHz linear array probe, greatly enhances our ability to interrogate flat plate specimens. The final section of this Progress Report describes a woven composite plate specimen that has been specially machined to include intentional flaws. This woven composite specimen will allow us to assess the feasibility of applying linear array imaging technology to the inspection and characterization of complex textile composite materials.

We anticipate the results of this on-going investigation may provide a step toward the development of a rapid, real-time, and portable method of ultrasonic inspection and characterization based on linear array technology.

Detection of Intentionally Disbonded Regions in Bonded Aluminum Plates Using a 7.5 MHz Linear Array

Introduction

Current concern for ensuring the air-worthiness of the aging commercial air fleet has prompted the establishment of broad-agency programs to develop NDT technologies that address specific aging-aircraft issues.^{1,2} One of the crucial technological needs that has been identified is the development of rapid, quantitative systems for depot-level inspection of bonded aluminum lap joints on aircraft.¹⁻³ Research results for characterization of disbond and corrosion based on normal-incidence pulse-echo measurement geometries are showing promise, but are limited by the single-site nature of the measurement which requires manual or mechanical scanning to inspect an area.⁴⁻⁷ One approach to developing efficient systems may be to transfer specific aspects of current medical imaging technology to the NDT arena. Ultrasonic medical imaging systems offer many desirable attributes for large scale inspection. They are portable, provide real-time imaging, and have integrated video tape recorder and printer capabilities available for documentation and post-inspection review. Furthermore, these systems are available at a relatively low cost (approximately \$50,000 to \$200,000) and can be optimized for use with metals with straight-forward modifications. As an example, ultrasonic phased-array and linear array imaging technology, which was first developed for use in the medical industry, has been successfully implemented for some NDT applications by other investigators.⁸⁻¹⁰

In this section of the Progress Report we explore the feasibility of implementing medical linear array imaging technology as a viable ultrasonic-based nondestructive evaluation method to inspect and characterize bonded aluminum lap joints. We present images, obtained using an unmodified medical ultrasonic imaging system, of two epoxy-bonded aluminum plate specimens, each with intentionally disbonded regions. These images are compared with corresponding conventional ultrasonic contact transducer measurements in order to assess whether these images can detect disbonded regions and provide information regarding the nature of the disbonded region. The results of this investigation may provide a step toward the development of a rapid, real-time, and portable method of adhesive bond inspection and characterization based on linear array technology.

Background

The images of the bonded aluminum specimens presented below were obtained using an unmodified, commercially-available Hewlett-Packard SONOS 1500 medical imaging system. Because of the nature of detecting disbanded regions in relatively thin aluminum specimens, the SONOS 1500 imaging system was operated in a mode normally employed to image peripheral blood vessels in a clinical setting. In this peripheral vascular imaging mode, the SONOS 1500 utilizes a linear array of ultrasonic transducer elements as the interrogating probe. A B-scan (cross-sectional) image of the object under interrogation is formed by sequentially transmitting and receiving with groups of transducer elements across the array. Each transmission of an ultrasonic pulse and the subsequent reception of the returned signals by a specific group of transducers represents one ultrasonic A-line in a direction normal to the array. The B-scan image is produced from a series of A-lines across the aperture of the array. Transmit and receive focus is achieved by selecting the appropriate groups of transducer elements and adjusting the relative time of transmit and receive between them. A depth-dependent gain (time-gain compensation or TGC) can be applied to the received ultrasonic signals to reduce the effects of the inherent attenuation of the specimen on the displayed B-scan image.

The B-scan images obtained with the linear array are processed and displayed in a conventional manner. Each received rf A-line signal is mixed to an intermediate frequency, amplified, rectified, and low-pass filtered. The B-scan image, formed from the amplitude envelopes of a series of A-line signals, is logarithmically compressed and displayed as a gray scale image on a dB scale. In general, each B-scan image obtained with a linear array is a cross-sectional representation of the amplitude of the reflected (scattered) ultrasonic signals, in the plane of the array, throughout the depth of the specimen under interrogation. However, interpretation of the images obtained from layered solids may be expected to be more complex than in tissue because of the presence of strong reverberations and possible mode conversions.

Because the SONOS 1500 system was intended to image specific peripheral blood vessels, it was not possible to change the depth setting of the images to more closely correspond to the thickness dimensions of the bonded aluminum plates. Furthermore, because the thicknesses of the bonded aluminum plate specimens were relatively small and the velocity of sound in aluminum is relatively large (compared to that of tissue), the images obtained with the SONOS 1500 system represent the echo-decay patterns of many round-trip echoes in the plates. Nonetheless, the B-scan images of echo decay patterns in

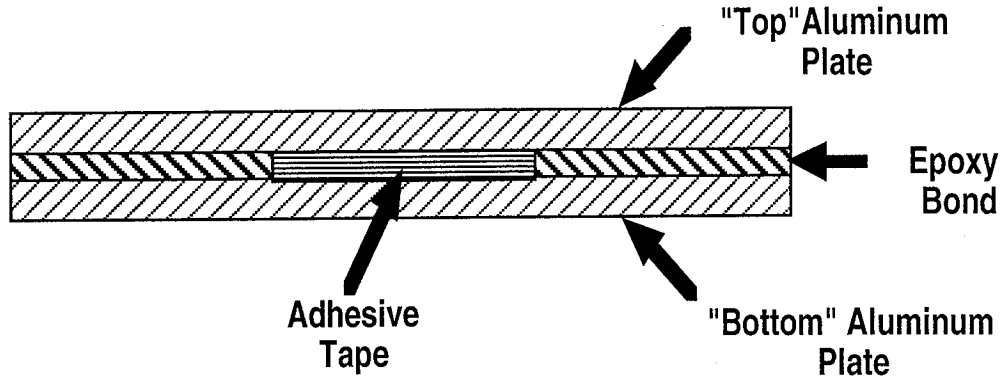


Figure 1 - Cross-sectional representation of bonded aluminum plate specimen.

bonded aluminum plates appears to represent a viable mode for identifying regions of disbond as will be further discussed below.

Specimens

Both of the bonded aluminum plate specimens interrogated in this investigation were 4.9 cm (1.9 inches) in width by 9.6 cm (3.8 inches) in length. Specimen #1 was constructed using two identical aluminum plates of 0.16 cm (0.063 inch) in thickness; whereas specimen #2 was constructed using one aluminum plate of 0.16 cm (0.063 inch) in thickness and one aluminum plate of 0.23 cm (0.090 inch) in thickness. In each case the specimens were constructed with an area of layered adhesive tape to simulate a disbanded region. These bonded plate specimens were produced by layering adhesive tape in specific areas on one of the plates (referred to as the "bottom" plate) until the layered tape was a specific thickness. For the specimens used in this investigation, layers of masking tape were first applied to the "bottom" plate followed by layers of clear cellophane tape. Epoxy was applied to the "bottom" plate which had the layered adhesive tape attached and a "top" aluminum plate was applied. After the epoxy had cured the specimens were machined to the final length and width dimensions leaving only one area of simulated disbond transversing the width of the specimen near the center. The width of the disbanded region was 1.27 cm (0.5 inch) for specimen #1 and 2.54 cm (1 inch) for specimen #2. Figure 1 illustrates how these specimens were constructed. Specimen #1 had an epoxy bond thickness of 0.03 cm (0.012 inch) and specimen #2 had an epoxy bond thickness of 0.04 cm (0.016 inch). The measured total thicknesses of the resultant specimens were 0.347 cm (0.136 inches) and 0.424 cm (0.167 inches) for specimens #1 and #2, respectively. In the final configuration the "top" aluminum plate of each specimen was in direct adhesive contact with the epoxy bond everywhere except over the region of the disbond (layered

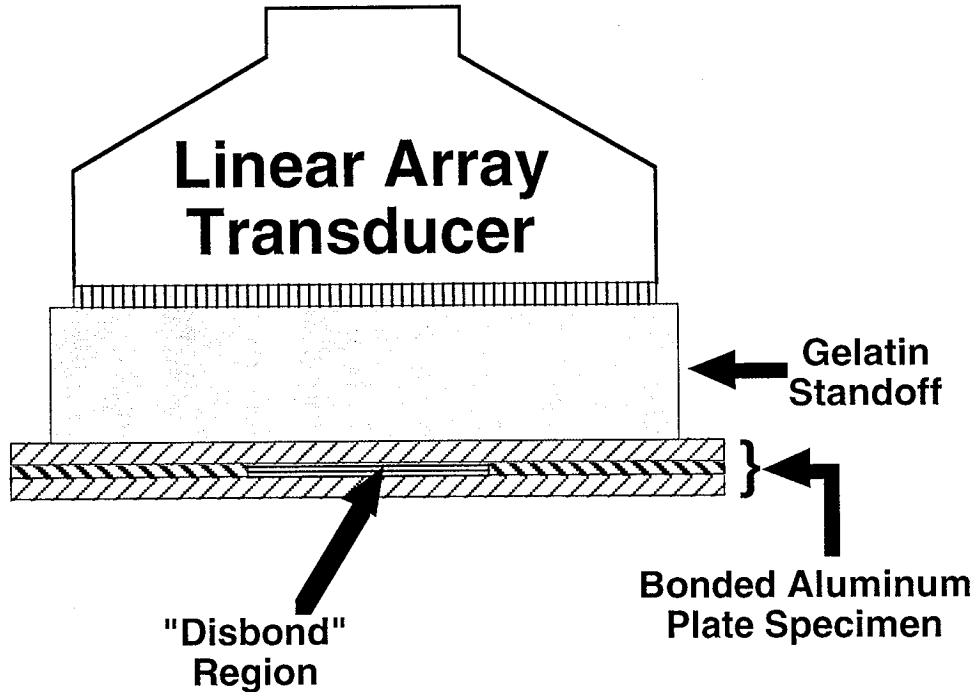


Figure 2 - Configuration of linear array transducer and gelatin standoff for obtaining images of the disbonded region in the bonded aluminum plate specimens.

tape). The "bottom" plate was also in direct contact with the epoxy outside the disbond region and in contact with the adhesive side of the masking tape in the region of disbond.

Linear Array Images

The aluminum plate specimens were imaged with the Hewlett-Packard SONOS 1500 medical imaging system in the peripheral vascular imaging mode described above. For these measurements a nominal 7.5 MHz center-frequency linear array probe was used with an overall length of 3.9 cm (1.5 inches). Each aluminum plate specimen was imaged with a gelatin stand-off approximately 2.54 cm (1 inch) in thickness between the linear array and specimen as illustrated in Figure 2. The gelatin stand-off was implemented to bring the front surface echo of the aluminum specimens closer to the center of the image. Each specimen was imaged with the axis of the linear array along the long axis (length dimension) of the specimen such that the linear array straddled the disbond region. The SONOS 1500 imaging system was configured such that the transmit power level was kept constant for all measurements and the same depth dependent gain (time-gain compensation) was applied to all depth segments and kept constant between the specimens. The video compression was adjusted to optimize the image contrast and remained constant for each

Linear Array Image

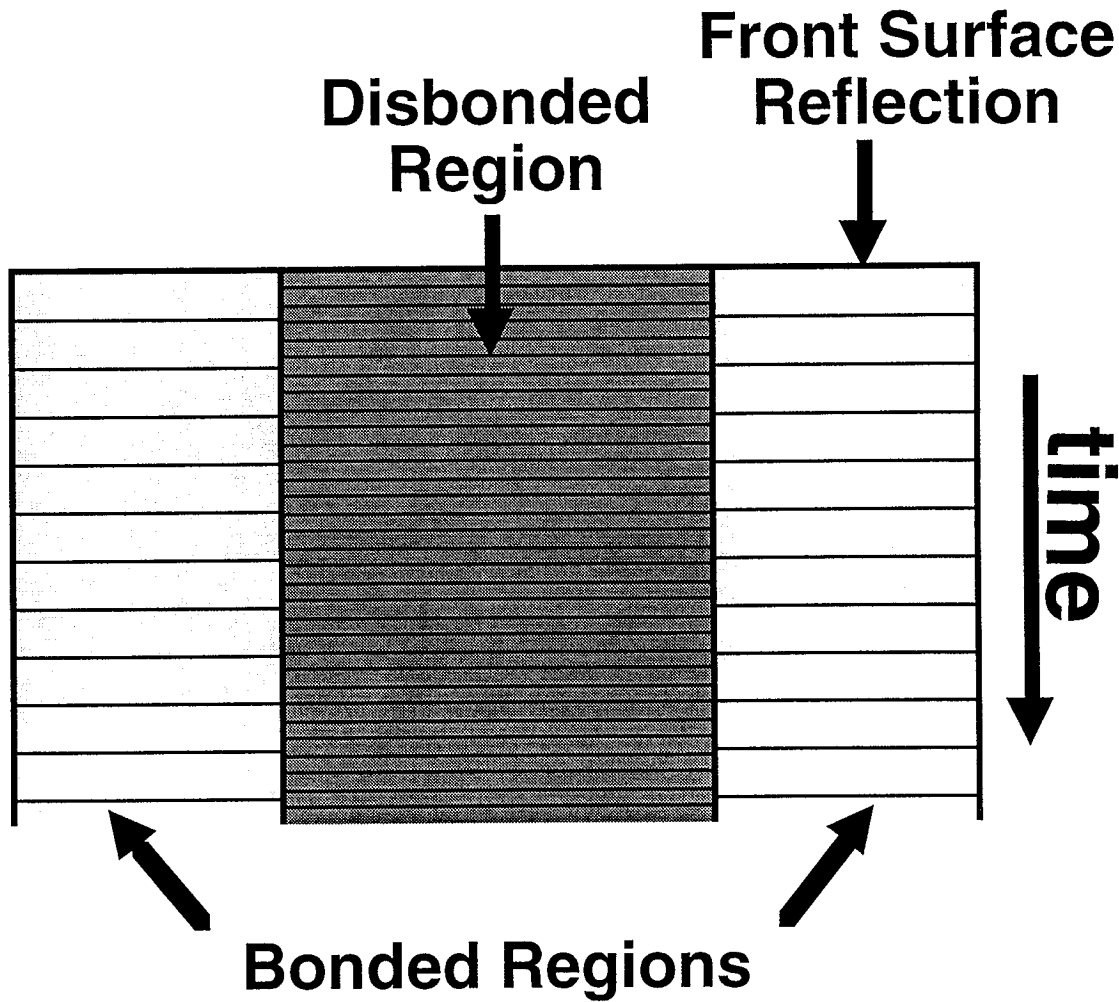


Figure 3 - Illustration showing how to interpret the images of the bonded aluminum specimens obtained with the linear array system.

specimen interrogated. The disbonded region and surrounding regions of each specimen were imaged from both sides of the specimen; i.e., each specimen was imaged from the aluminum plate side in contact with the adhesive of the masking tape ("bottom" side) as well as the side with no masking tape adhesive on the plate ("top" side).

Figure 3 illustrates how to interpret the images of the bonded aluminum specimens obtained with the linear array system. The images obtained from both sides of the specimen straddle the disbond region. The disbonded region is represented by the more

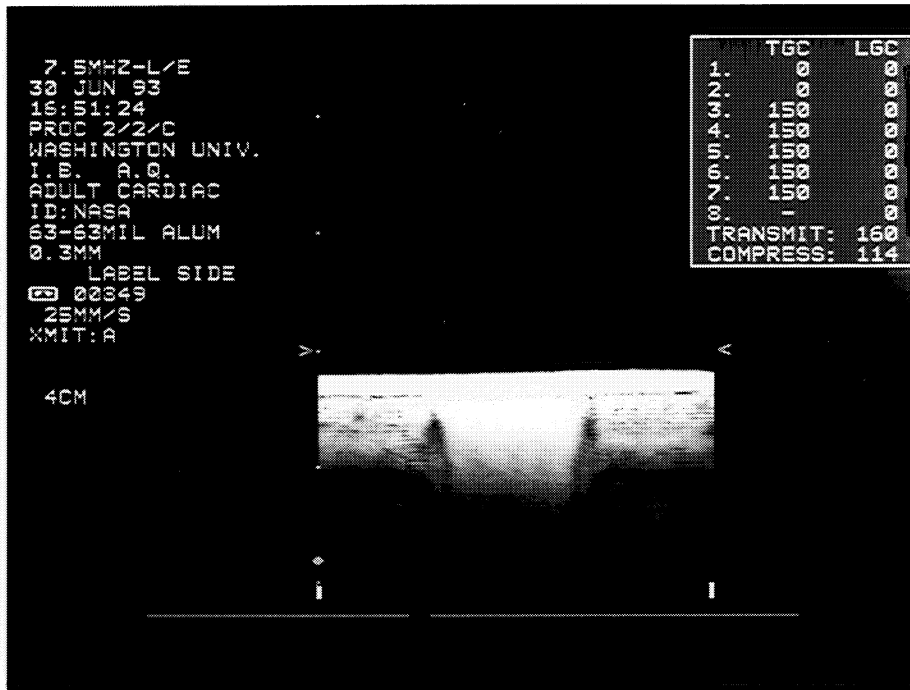
darkly shaded area in Figure 3. On either side of the disbonded region is the well-bonded region, depicted as the more lightly shaded region in Figure 3. Recall that these images are composed of many reverberations of the ultrasonic signal in the specimen and do not represent a single cross-section.

Figure 4 shows the linear array images over the disbonded region for specimen #1 from both sides. In Figure 4a the region of disbond can be clearly distinguished from the surrounding well-bonded region in the image. This image was obtained from the "bottom" side of the specimen where the masking tape was adhered to the aluminum plate. As described above, the B-scan image represents the returned signals from many round-trip echoes (reverberations) inside the specimen and does not represent a single cross-section through the depth of the specimen. Comparing the disbonded region with the surrounding bonded region in this image it appears that different echo decay patterns can be observed. The echo decay pattern corresponding to the disbonded region appears "brighter" than the surrounding regions and appears to monotonically decrease in brightness as time increases. Furthermore, the individual echo patterns do not appear as prominent in the disbond region as those observed in the surrounding regions thus giving the disbond region a more "smooth" appearance. The brightness of the echo pattern from the well-bonded region appears to be more modulated and the individual echoes appear more prominently.

Figure 4b shows the B-scan image of the disbonded region of specimen #1 obtained from the "top" side of the specimen. In this image the region of disbond can again be clearly distinguished from the surrounding well-bonded region although it appears much different than that observed when imaged from the "bottom" side of the specimen (Figure 4a). The image in Figure 4b shows the disbonded region to be much darker than the surrounding well-bonded regions. This appears to be indicative of a higher attenuation of ultrasound in the disbond region and hence a more rapid rate of echo decay when imaged from the "top" side. Although the disbond region looks very different when Figures 4a and 4b are compared, the well-bonded regions appear to be very similar in the two images. We would expect the images from the well-bonded regions to be very similar when imaged from both sides of the specimen because the thickness of each of the aluminum plates is the same and hence the ultrasound propagates along the same path in both cases.

Figure 5 displays the B-scan images obtained from specimen #2. Figure 5a shows the B-scan image obtained when specimen #2 is interrogated from the "bottom" side of the specimen; the side in which the masking tape was adhered to the "bottom" plate. The

a)



b)

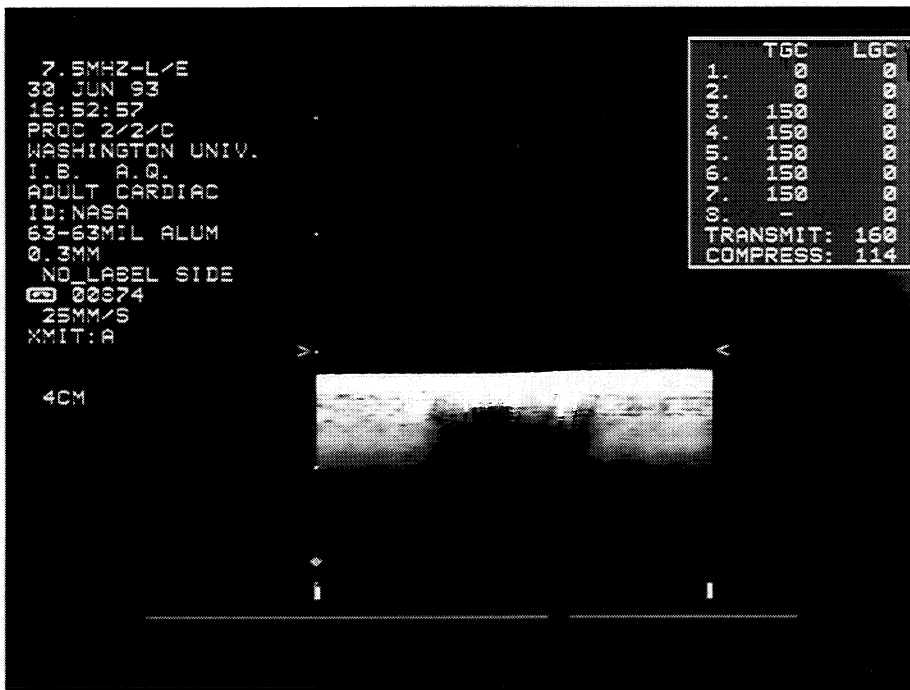
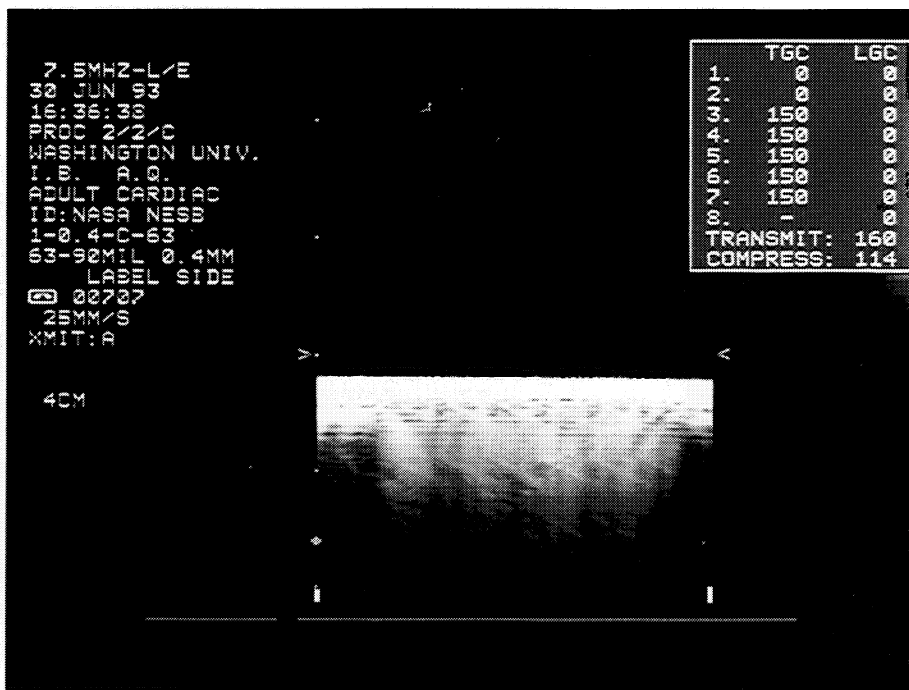


Figure 4 - Linear array images over the disbonded region for specimen #1. Figure 4a shows the B-scan image of the disbonded region obtained from the "bottom" side of the specimen. Figure 4b shows the B-scan image of the disbonded region obtained from the "top" side of the specimen.

a)



b)

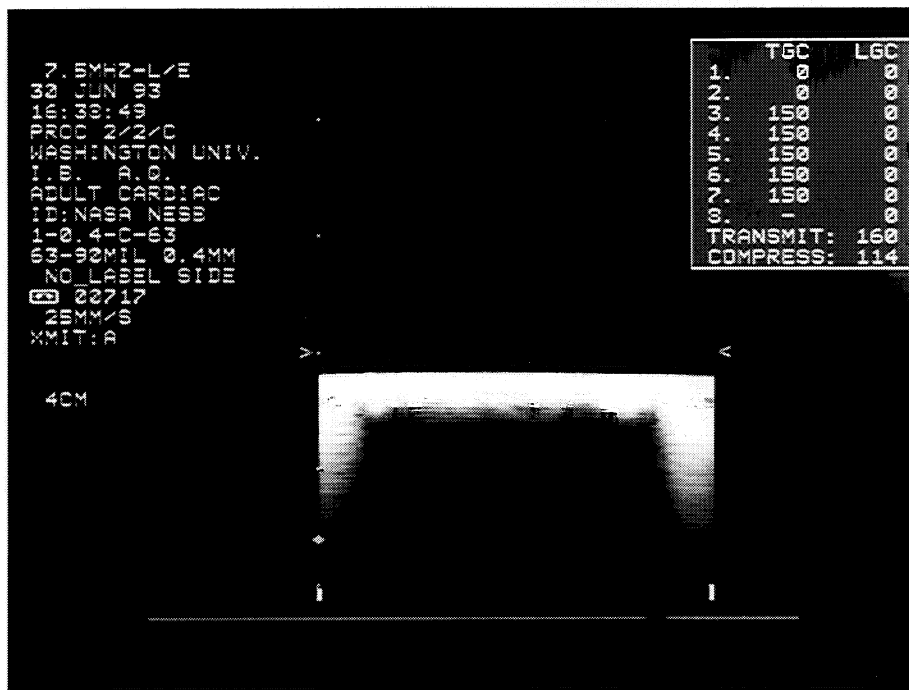


Figure 5 - Linear array images over the disbonded region for specimen #2. Figure 5a shows the B-scan image of the disbonded region obtained from the "bottom" side of the specimen. Figure 5b shows the B-scan image of the disbonded region obtained from the "top" side of the specimen.

image from the "top" side of the specimen is depicted in Figure 5b. The disbond region is again clearly distinguished from the surrounding well-bonded regions in both of these figures. Many of the same features are apparent in these images of specimen #2 as were observed in the images of specimen #1 (Figure 4); e.g., the disbond region appears "brighter" compared to the well-bonded region when specimen #2 is imaged from the "bottom" side (Figure 5a) and much darker than the well-bonded region when imaged from the "top" side (Figure 5b).

There are some interesting differences between the images obtained from specimen #1 and the images obtained from specimen #2 in the well-bonded regions. In contrast to that observed for specimen #1, the echo patterns from the well-bonded regions do not look the same when specimen #2 is interrogated from the "bottom" compared to the images obtained from the "top". The difference in the observed echo pattern corresponding to well-bonded regions may be related to the different thickness of aluminum plate present at the surface of interrogation. The sequence in which a transmitted ultrasonic pulse encounters an aluminum/epoxy interface is different for the two sides of specimen #2. Furthermore, the images of the well-bonded regions of specimen #2 do not appear to have the same modulation pattern of image brightness as observed for specimen #1.

Contact Transducer Measurements

In order to interpret the images of the bonded aluminum plate specimens obtained with the linear array, single element contact transducer measurements were performed. Ultrasonic rf A-lines from the bonded and disbonded regions of each specimen were obtained from each side of each specimen. Pulse-echo measurements were made with a broadband, 0.25-inch diameter, 25 MHz contact transducer (KB Aerotech - Alpha DFR) with a 0.98 cm (0.375 inch) delay line. A Panametrics 5800 computer controlled pulser/receiver was used to generate the broadband excitation pulse and to amplify the returned ultrasonic signal. The returned rf signal was taken from the Panametrics 5800 receiver output and sent to a Tektronix TDS 520 digitizing oscilloscope. Signals were digitized at a rate of 250 megasamples/second with 8-bit resolution over a total record length of 2500 points. The digitized rf signals were stored on a Macintosh IIfx for off-line analyses.

A set of at least three rf A-line signals were digitized from each region (bonded or disbonded) on each side ("bottom" or "top") of each specimen. The digitized signals of each set were very similar although small variations in signal size were observed. These

Specimen #1

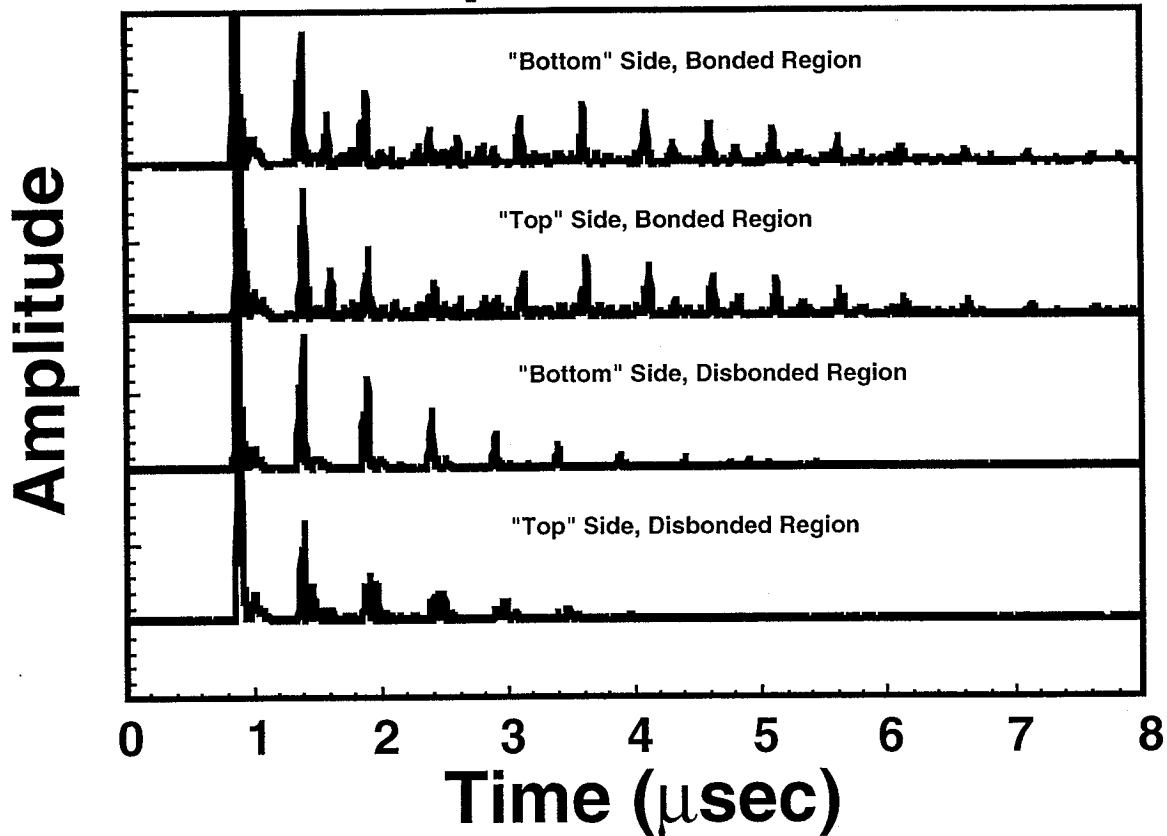


Figure 6 - Representative rf A-line amplitude signals obtained from each of the specific regions of specimen #1.

small variations appear to be related to the variable degree of pressure one exerts when pressing the contact transducer on the surface of the specimen. Figure 6 depicts one representative rf A-line signal (amplitude) obtained from each of the specific areas of specimen #1. In this figure the rf A-lines representing the bonded region from both sides of specimen #1 appear to be very similar. This is consistent with the images in Figure 4 above and is a result of the inherent symmetry of this bonded aluminum plate specimen. There appears to be a modulation of the echo amplitudes in the rf A-line from the well-bonded region obtained from both sides of the specimen. This modulation may be the result of interference between signals returning from the various interfaces for the particular aluminum plate thickness and epoxy bond thickness of this specimen. These A-lines from the well-bonded regions show a significant amount of signal between the larger interface echoes that are due to multiple reverberations within the specimen.

Figure 6 shows that the amplitude echo decay pattern from the disbonded region of the "bottom" side of specimen #1 has a different shape than the rf A-lines obtained from the well-bonded region. The echo amplitudes from the disbonded region appear to decrease monotonically in time. Time between interface echoes in this region is approximately 0.50 μ sec, which corresponds to a round-trip distance of 0.32 cm in aluminum, twice the thickness of the bottom aluminum plate. Furthermore, it appears that there is not as much backscattered signal occurring between the interface echoes, suggesting that sound does not propagate easily beyond the aluminum-tape interface from this side. The echo decay pattern from the disbonded region of specimen #1 obtained from the "top" side is also shown in Figure 6. This echo decay pattern demonstrates an apparent monotonic decrease in echo amplitude with time and it appears that this decrease in amplitude is at a greater rate than that observed for the disbonded region when measured from the "bottom" side. This A-line, obtained from the disbonded region of the "top" side, appears to have a significant amount of signal after the larger interface echoes. We hypothesize that the observed differences between the rf A-lines obtained from the disbond region of the "top" plate and the rf A-lines obtained from the disbond region of the "bottom" plate may be a consequence of the specific nature of the disbond/aluminum interfaces occurring at the "top" and "bottom" plates.

Figure 7 depicts the corresponding representative rf A-line signals (amplitude) obtained from each of the specific areas of specimen #2. The echo decay patterns for the well-bonded region from the two sides of the specimen ("bottom" and "top") do not appear to be the same as they did for specimen #1. This is to be expected because the "bottom" and "top" aluminum plates are of different thicknesses for specimen #2 and the ultrasound propagates through the different layers of the specimen in a different sequence. The rf A-lines from this well-bonded region of specimen #2 do not appear to demonstrate such a strong modulation of the echo amplitudes with time. These A-lines show a significant amount of signal between the larger interface echoes, similar to that observed for specimen #1, which is due to multiple reverberations within the specimen.

As was observed for specimen #1, Figure 7 shows that the amplitude echo decay pattern from the disbonded region of the "bottom" side of specimen #2 has a different shape than that observed for the well-bonded region. The echo amplitudes from the disbonded region appear to decrease monotonically in time for specimen #2 as they did for specimen #1. Measurement of the time between interface echoes in this region provides a round-trip time of approximately 0.72 μ sec, which corresponds to a round-trip distance of

Specimen #2

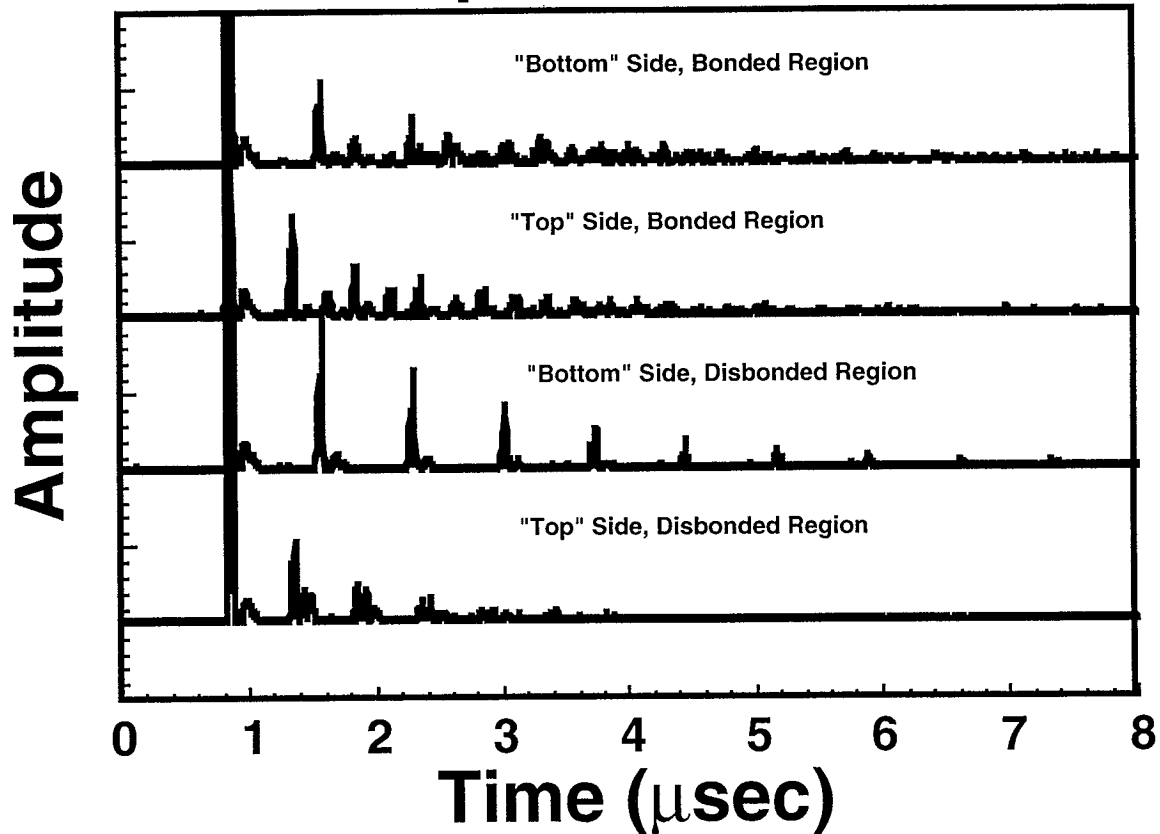


Figure 7 - Representative rf A-line amplitude signals obtained from each of the specific regions of specimen #2.

0.45 cm in aluminum, twice the thickness of the "bottom" aluminum plate of specimen #2. Furthermore, as was observed for specimen #1, it appears that there is not as much signal occurring between the interface echoes, suggesting that sound does not propagate easily beyond the aluminum-tape interface from this side. The echo decay pattern from the disbonded region of specimen #2 obtained from the "top" side is also shown in Figure 7. As found for specimen #1, this echo decay pattern also appears to demonstrate a decrease in signal amplitude at a greater rate than that observed for the disbonded region when measured from the "bottom" side. Again this is indicative of a greater attenuation of the signal and may be related to the specific nature of the aluminum/disbond interface. As was observed in specimen #1, there appears to be a significant amount of scattered signal after the larger interface echoes when compared with the signal obtained from the "bottom" side.

Discussion

The results presented above, showing the images of the bonded aluminum plate specimens obtained with the linear array and the corresponding ultrasonic rf A-lines obtained with a contact transducer, suggest that linear array imaging can play a useful role in detecting disbonded regions and providing information describing bond interface characteristics. The disbonded region was easily discernible from the well-bonded region in the images obtained from either side of each specimen. Images of both specimens show that the disbonded region looks much different than the surrounding well-bonded region when the images obtained from the "bottom" of the specimen are compared with those obtained from the "top". The relatively "bright" disbond region observed when the specimens are imaged from the "bottom" side and the "dark" disbond region observed when the specimens are imaged from the "top" side agree with the corresponding echo decay patterns obtained with the contact transducer; i.e., a relatively higher attenuation associated with the disbonded region when interrogated from the "top" when compared with the results obtained from the "bottom". Subsequent destructive analysis of the specimens showed that the "bottom" plate was in direct contact with the adhesive of the masking tape (as expected) but the "top" plate had a thin substance adhered to it. These results suggest that the images obtained with the linear array may convey information regarding the characteristics of the interface between the aluminum and the disbond.

Images of the well-bonded regions of both specimens obtained with the SONOS 1500 linear array are also consistent with the contact transducer data. The modulation of the brightness of the well-bonded region in the images of specimen #1 agree well with the observed modulations in the echo decay patterns obtained with the contact transducer and the similarity between the images of the bonded region from both sides of specimen #1 are consistent with the similar nature of the echo decay patterns from both sides. Images of specimen #2, which has aluminum plates of different thicknesses, are also consistent with the measured rf A-lines of this specimen. Images of specimen #2 show that the well-bonded region appears different when interrogated from the "bottom" side and compared with the image from the "top" side. This difference between the two sides is also evident in the measured echo decay patterns obtained from the two sides. The relatively longer echo decay pattern (lower attenuation) corresponding to the disbonded region of the "bottom" side of specimen #2 compared to the well-bonded region is also very evident in the image of that side.

The images of the bonded aluminum plate specimens and the corresponding agreement with contact transducer measurements suggest that linear array technology may provide a viable means to detect disbanded regions in bonded aluminum joints. Furthermore, these images may provide useful information regarding the nature of the disbanded region. It appears that medical linear array imaging technology may offer a useful means to develop a rapid, real-time, and portable method of adhesive bond inspection and characterization.

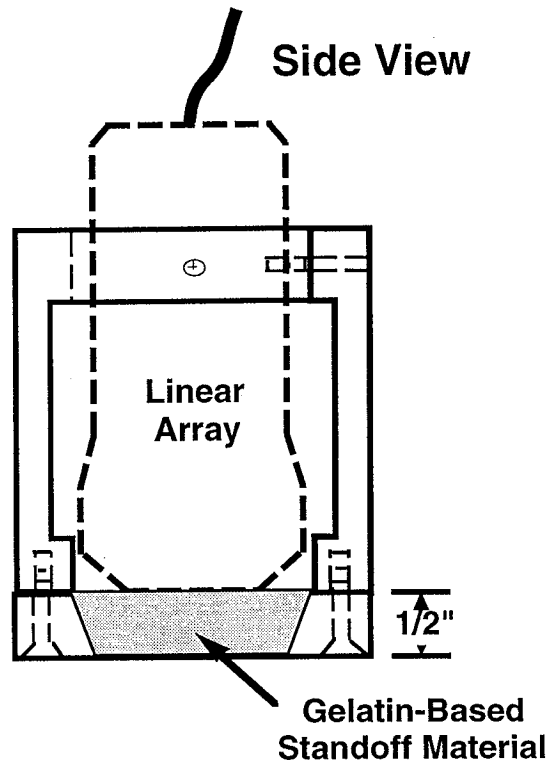


Figure 8 - Standoff/delay fixture designed for use with the 7.5 MHz linear array probe.

Standoff/Delay Fixture for the 7.5 MHz Linear Array

In order to facilitate the inspection of specimens with the Hewlett-Packard SONOS 1500 medical imaging system a standoff/delay fixture was designed for use with the 7.5 MHz linear array probe. This standoff/delay fixture, illustrated in Figure 8, clamps around the Hewlett-Packard linear array probe. The use of the standoff/delay fixture in the inspection of the test specimens allows the specimen to be placed in a region away from the face of the linear array and thus reduces the effects of transducer ring-down and near field artifact. This is especially important when investigating relatively thin specimens with relatively large inherent ultrasonic velocities (compared to tissue). Furthermore, the use of this standoff/delay fixture allows the operator to keep the linear array probe perpendicular to the specimen under interrogation as the array is translated across the surface. The clamping screws allow precise alignment of the probe with respect to the surface. The standoff/delay material was a NASA developed, gelatin-based, tissue-mimicking material, with a velocity of sound close to that of tissue.¹¹

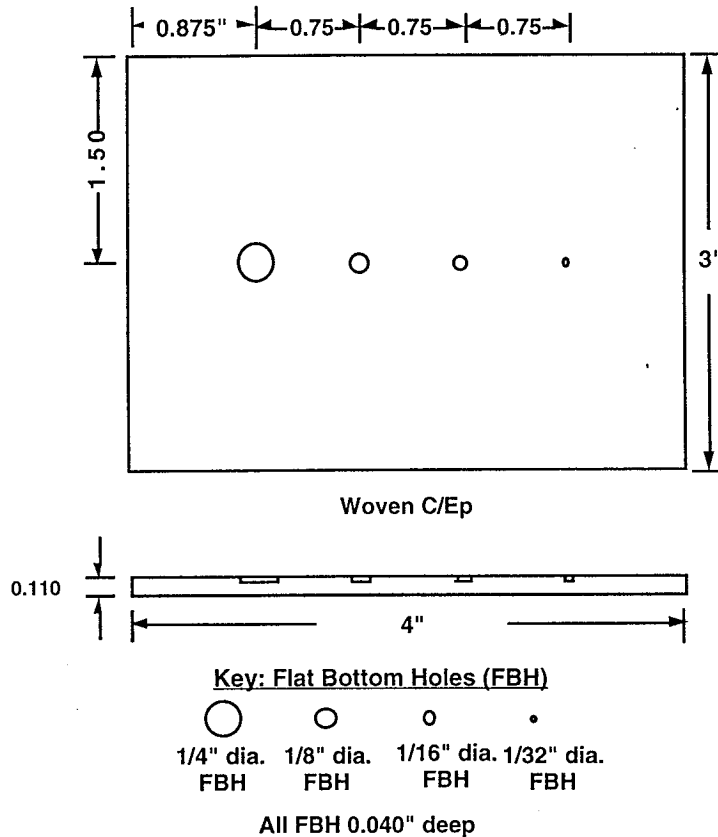


Figure 9 - Woven composite plate specimen specially machined to include four flat-bottom holes of specific diameters.

A Woven Composite Plate with Flat-Bottom Holes to Simulate Flaws

In order to assess the feasibility of applying linear array imaging technology to the inspection and characterization of complex textile composite materials, a woven composite plate specimen has been specially machined to include intentional flaws. An eight-ply, 5-harness, woven carbon/epoxy composite plate, with dimensions of 3.0 inches by 4.0 inches and a thickness of 0.110 inches, was machined to include four flat-bottom holes of specific diameters. Figure 9 shows a schematic drawing of the woven composite plate. This Figure shows the flat-bottom holes, with diameters of 1/4-inch, 1/8-inch, 1/16-inch, and 1/32-inch, were machined to a depth of 0.040 inches along a line through the center of the specimen. The flat-bottom holes have an inter-hole spacing of 3/4-inch as indicated in the Figure. These flat-bottom holes are intended to simulate flaws of different sizes that may occur during the production of the a composite structure or might occur after

implementation of a composite structure in the field. The 7.5 MHz linear array will be used to interrogate this specimen and determine how well each of the individual flaws can be resolved. Furthermore, we will interrogate the composite plate with a conventional single-element contact transducer and the ability to find these simulated flaws will be compared.

References

1. S.N. Bobo, "The Aging Aircraft Fleet: A Challenge for Nondestructive Inspection"(D.O.T.a.D.E. Chimentis, Eds. (Plenum Publishing Corporation, Brunswick, ME, Published 1990), Vol. 9, pp. 2097-2109.
2. C. Seher and A.L. Broz, "National Research Program for Nondestructive Inspection of Aging Aircraft," *Materials Evaluation* **49**, 1547-1550 (1991).
3. F.A. Iddings, "Large-Area Aircraft Scanner"(D.O.T.a.D.E. Chimentis, Eds. (Plenum Publishing Corporation, Brunswick, ME, Published 1992), Vol. 11, pp. 2233-2240.
4. T.C. Patton and D.K. Hsu, "Ultrasonic NDE of Adhesive and Sealant Bonded Aluminum Lap Joints"(D.O.T.a.D.E. Chimentis, Eds. (Plenum Publishing Corporation, Brunswick, ME, Published 1992), Vol. 11, pp. 1299-1306.
5. D.K. Hsu, M.S. Hughes, and T.C. Patton, "Ultrasonic Scans Using Low Frequency Unresolved Echoes"(D.O.T.a.D.E. Chimentis, Eds. (Plenum Publishing Corporation, Brunswick, ME, Published 1993), Vol. 12, pp. 1595-1602.
6. M.N. Abedin, D.R. Prabhu, W.P. Winfree, and P.H. Johnston, "A Comparative Study of Experimental and Simulated Ultrasonic Pulse-Echo Signals from Multilayered Structures"(D.O.T.a.D.E. Chimentis, Eds. (Plenum Publishing Corporation, Brunswick, ME, Published 1992), Vol. 11, pp. 1959-1966.
7. M.N. Abedin, P.H. Johnston, and D.R. Prabhu, "Disbond Detection Using Peak Amplitude of Pulse-Echo Signals for Various Thicknesses and Transducer Frequencies"(D.O.T.a.D.E. Chimentis, Eds. (Plenum Publishing Corporation, Published 1993), Vol. 12, pp. 1539-1546.
8. R. Dunki-Jacobs and L.J. Thomas, "Real-Time B-Scan Ultrasonic Imaging Using a Digital Phased Array System for NDE"(D.O.T.a.D.E. Chimentis, Eds. (Plenum Publishing Corporation, Brunswick, ME, Published 1992), Vol. 11, pp. 805-812.
9. H. Wustenberg, B. Rotter, H.P. Klanke, and D. Harbecke, "Ultrasonic Phased Arrays for Nondestructive Inspection of Forgings," *Materials Evaluation* **51**, 669-812 (1993).
10. G.J. Posakony, "Acoustic Imaging - A Review of Current Techniques for Utilizing Ultrasonic Linear Arrays for Producing Images of Flaws in Solids""((Published 1978), Vol. 29, pp. 53 -69.
11. "Tissue-Simulating Gel for Medical Research", NASA Langley Research Center, Report Number: LAR-14036, (1993).